



# Evaluation of natural radioactivity in soils of Konya (Turkey) and estimation of radiological health hazards

Selin Özden · Serpil Aközcan Pehlivanoğlu · Osman Günay

Received: 18 August 2023 / Accepted: 18 November 2023 / Published online: 23 November 2023  
© The Author(s), under exclusive licence to Springer Nature Switzerland AG 2023

**Abstract** Surface soil samples were collected from Konya, Turkey and natural activity concentrations were determined using the  $\gamma$ -ray spectroscopy system with HPGe detector. The activity concentrations of  $^{226}\text{Ra}$ ,  $^{232}\text{Th}$  and  $^{40}\text{K}$  were found to vary from  $14.07 \pm 0.71 \text{ Bq kg}^{-1} \text{ dw}$  to  $67.27 \pm 1.62 \text{ Bq kg}^{-1} \text{ dw}$ ,  $10.19 \pm 2.60 \text{ Bq kg}^{-1} \text{ dw}$  to  $46.09 \pm 0.76 \text{ Bq kg}^{-1} \text{ dw}$  and  $107.87 \pm 13.32 \text{ Bq kg}^{-1} \text{ dw}$  to  $605.95 \pm 11.34 \text{ Bq kg}^{-1} \text{ dry weight (dw)}$ , respectively. The radiological hazard parameters such as  $R_{\text{eq}}$ , D, AEDE, ELCR, AGDE,  $H_{\text{ex}}$ ,  $H_{\text{in}}$ , and  $I_{\text{r}}$  evaluated the radiological risk for the public and environment. The mean values of D, AEDE and ELCR are lower than the world average value of  $57 \text{ nGy h}^{-1}$ ,  $70 \mu\text{Sv y}^{-1}$ ,  $0.29 \times 10^{-3}$  respectively. The activity concentration distribution maps of  $^{226}\text{Ra}$ ,  $^{232}\text{Th}$  and  $^{40}\text{K}$  and the radiological maps of the radiological hazard parameters were plotted using the Surfer programme. Cluster analysis was carried out to indicate the similarity between the variables.

**Keywords** Radiation hazard · Soil · Radioactivity · Natural radioactivity · Cancer risk

## Introduction

People are unavoidably exposed to radiation throughout their lives. Naturally occurring radioactive materials (NORMs) contribute greatly to radiation. The radioactivity due to NORMs is detrimental to human health and causes environmental pollution. NORMs are present in soil, rock, water, air, sediment and sand. In soil, potassium ( $^{40}\text{K}$ ), uranium ( $^{238}\text{U}$ ), thorium ( $^{232}\text{Th}$ ) and their decay products are known primary NORMs and cause an increase in radioactivity levels. Particularly,  $^{226}\text{Ra}$ ,  $^{232}\text{Th}$  and  $^{40}\text{K}$  induce the natural background radiation in soil and it's approximately 80% of the total radiation dose a person is exposed to in a year (Ibraheem et al., 2018). Knowing the radioactivity concentrations of NORMs in soil provides useful information in determining environmental radioactivity.

The level of human exposure depends on the geological morphology of the soil. Therefore, soil radioactivity concentration analysis plays a very significant role in determining the level of exposure of human beings (Tiomene et al., 2023). Exposure to NORMs causes many health problems such as lung diseases, leukemia and cancers (Uosif & El-Taher, 2008). Soils are evermore a source of radiation for all living beings because NORMs in soil transfer to plants, water, air, animals, humans, etc. (Murugesan et al., 2011; Özden & Aközcan, 2021).

---

S. Özden (✉) · S. A. Pehlivanoğlu  
Department of Physics, Kirklareli University, Kirklareli,  
Turkey  
e-mail: selinnozden@gmail.com

S. A. Pehlivanoğlu  
e-mail: serpil.akozcan@klu.edu.tr

O. Günay  
Department of Biomedical Engineering, Yildiz Technical  
University, İstanbul, Turkey  
e-mail: ogunay@yildiz.edu.tr

The NORMs' distribution in the soil differs from area to area depending on the usage of phosphate fertilizer, mining activities, industrial activities, geological structure and geographical formation (Özden & Aközcan, 2021; Akkurt et al., 2022; İçhedef et al., 2015). Recycled by-products used in industry increase natural radioactivity levels (Žak et al., 2010). In the geological structure of the earth, there are rock beds just below the soil layer of a certain thickness. These rock beds are estimated to cause terrestrial radioactivity. It is known that most of the gamma radiations originate from the surface layer (0–25 cm) (Küçükönder et al., 2023; UNSCEAR, 1993). The safety of a population is directly related to the activity concentration of  $^{226}\text{Ra}$ ,  $^{232}\text{Th}$  and  $^{40}\text{K}$  radionuclide concentrations in soil samples. Natural radionuclides in soils have attracted the attention of researchers because of the potential radiation exposure to humans and various studies have been carried out on this subject in different geological structures around the world (Al-Alawy et al., 2023; Alsaadi et al., 2023; Elsaman et al., 2022; Hafızoğlu, 2023; Özden, 2022; Özden & Aközcan, 2021; Pucha et al., 2023; Srinivasa et al., 2022).

The objective of this study is to indicate the natural radioactivity concentrations, the distribution of NORMs in soils in Konya, Turkey and also to evaluate the radiological parameters, namely, radium equivalent activity ( $Ra_{eq}$ ), absorbed gamma dose rate (D), annual effective dose equivalent (AEDE), external hazard index ( $H_{ex}$ ), internal hazard index ( $H_{in}$ ), excess lifetime cancer risk (ELCR), annual gonadal dose equivalent (AGDE) and gamma representative level index ( $I_\gamma$ ) due to soil samples. Cluster analyses were carried out to indicate the radionuclide distributions and to understand the relationships between parameters.

## Materials and methods

### Study area

Konya is the city with the largest surface area of Turkey. Konya is located on  $37^\circ 52' 28.7148''$  N and  $32^\circ 29' 35.358''$  E. It is estimated that Konya has a population of approximately 2.294.727 in 2022. The

landform with the largest area in Konya is plains and plateaus. These plateaus, which are covered with rich steppes, are important for the province's livestock and agriculture. In Konya, alluvial, colluvial, red brown and brown large soil groups are the commonly seen soil types. Alluvial soils are found in most of the residential areas of the city (Polat & Önder, 2004). The southwest of Konya has a volcanic geographic structure and NORMs are present in volcanic soils (Ibraheem et al., 2018; Solgun et al., 2021).

Samples were gathered at a depth of approximately 5–7 cm from the soil surface and a total of 26 different points in Konya were sampled (Fig. 1).

### Preparation of soil samples

After collected soil samples were brought to the laboratory in bags, unwanted materials such as gravel, stones, leaves, etc. were removed and soil samples were sieved through a 2-mm sieve. Before activity measurements, samples were dried in an oven at  $105^\circ\text{C}$  for 24 h, were placed inside polyethylene containers and kept in them for 1 month to achieve radioactive secular equilibrium (Murthuza et al., 2022).

### Activity measurements

Activity measurements of surface soil samples were performed using the  $\gamma$ -ray spectroscopy system with HPGe detector (ORTEC GEM70P4-95, USA) in Kırklareli University Central Research Laboratory. The HPGe detector has high resolution of 2.0 keV and 70% relative efficiency for 1.332 MeV gamma energy of Co-60. The calibrations were made using a standard mixed source with an energy range of 80 to 2500 keV (Isotope Products Laboratories) including known activity levels of  $^{210}\text{Pb}$ ,  $^{139}\text{Ce}$ ,  $^{109}\text{Cd}$ ,  $^{241}\text{Am}$ ,  $^{57}\text{Co}$ ,  $^{113}\text{Sn}$ ,  $^{203}\text{Hg}$ ,  $^{85}\text{Sr}$ ,  $^{88}\text{Y}$ ,  $^{137}\text{Cs}$ , and  $^{60}\text{Co}$  peaks.

The  $\gamma$ -spectra of the soil samples were acquired by counting for 160,000 s (44 h) and the Gamma-Vision-32 software program was used to obtain activity concentrations. The activity concentration of  $^{226}\text{Ra}$  was determined from  $\gamma$ -ray lines at, 351.9 keV for  $^{214}\text{Pb}$  and 609.3 keV for  $^{214}\text{Bi}$ , respectively. The content of  $^{232}\text{Th}$  was obtained from photo peaks of  $^{228}\text{Ac}$  at 911.2 keV and  $^{208}\text{Tl}$  at 583.1 keV. The

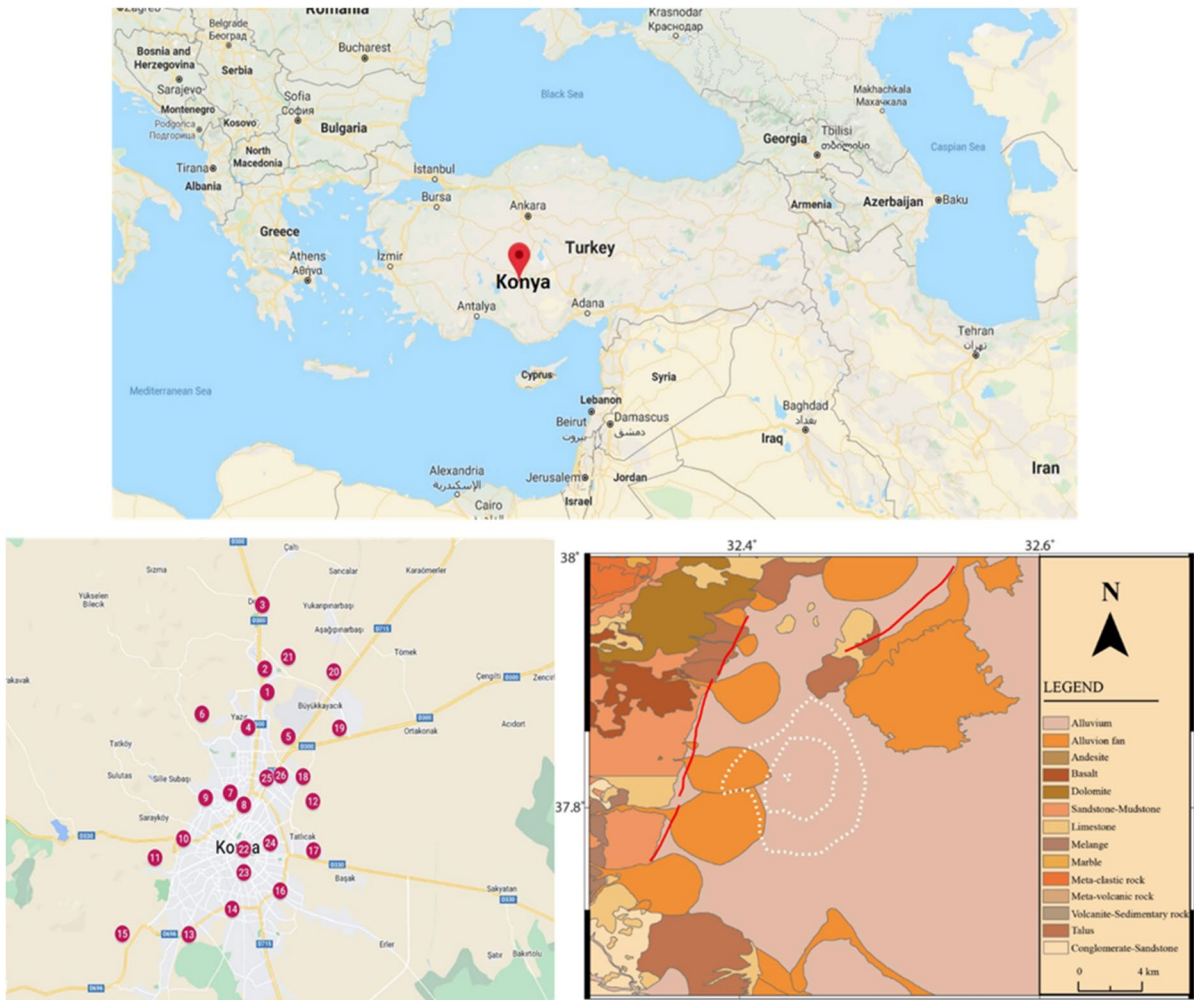


**Fig. 1** Map of the study area, sampling points and geological map of Konya (Şireci et al., 2021)

activity concentration of  $^{40}\text{K}$  was determined using an  $\gamma$ -ray line at 1460.8 keV (Aközcan et al., 2021; Özden & Aközcan, 2021).

The activity concentrations were calculated via the following equation (Hossain et al., 2010; Özden & Aközcan, 2021):

$$A(Bq\text{ kg}^{-1}) = \frac{CPS}{\epsilon m x I_{\gamma}} \tag{1}$$

where  $A$  ( $Bq\text{ kg}^{-1}$ ) is the activity concentration of a radionuclide in the surface soil sample, CPS is the net  $\gamma$  counting rate,  $\epsilon$  is the detection efficiency of a specific  $\gamma$ -ray,  $m$  is the mass of the measured sample and  $I_{\gamma}$  is the  $\gamma$ -ray emission probability.

#### Calculation of radiological hazard parameters

The radiological hazard parameters were calculated due to NORMs. In equations; the activity concentrations of  $^{226}\text{Ra}$ ,  $^{232}\text{Th}$  and  $^{40}\text{K}$  are defined by  $A_{Ra}$ ,  $A_{Th}$  and  $A_K$ , respectively.

#### Radium equivalent activity ( $Ra_{eq}$ )

NORMs are distributed nonuniformly in environmental media.  $Ra_{eq}$  is a proper parameter to compare activity concentrations in samples and has been determined to compare activity concentrations

of NORMs.  $Ra_{eq}$  was calculated in becquerels per kilogram using Eq. (2). (Beretka & Mathew, 1985).

$$Ra_{eq}(Bq\ kg^{-1}) = A_{Ra} + 1.43A_{Th} + 0.077A_K \quad (2)$$

In the equation, it is assumed that  $370\ Bq\ kg^{-1}$  of  $^{226}Ra$ ,  $259\ Bq\ kg^{-1}$  of  $^{232}Th$  or  $4810\ Bq\ kg^{-1}$  of  $^{40}K$  have the same gamma dose rate.

Absorbed gamma dose rate (D)

D ( $nGy\ h^{-1}$ ) in air through terrestrial  $\gamma$  radiation at 1 m above the ground was found by the following equation (UNSCEAR, 2000):

$$D\ (nGyh^{-1}) = 0.462A_{Ra} + 0.604A_{Th} + 0.0417A_K \quad (3)$$

0.462 is the conversion factor for  $^{226}Ra$ , 0.604 is the conversion factor for  $^{232}Th$  and 0.0417 is the conversion factor for  $^{40}K$ .

Annual effective dose equivalent (AEDE)

AEDE ( $\mu Sv\ y^{-1}$ ) caused by exposure to NORMs in surface soil samples was calculated using the following equation (Özden & Aközcan, 2021; Suresh et al., 2021):

$$AEDE\ (\mu Sv\ y^{-1}) = D\ (nGy\ h^{-1}) \times 8760\ (hy^{-1}) \times 0.2 \times 0.7\ (Sv\ Gy^{-1}) \times 10^{-3} \quad (4)$$

In the equation;  $D$ : the absorbed gamma dose rate ( $nGy\ h^{-1}$ ), 8760: hours per a year, 0.2: the outdoor occupancy factor, and 0.7: is the dose convention factor ( $Sv\ Gy^{-1}$ ). The equation was multiplied by  $10^{-3}$  to convert to  $\mu Sv$ .

Radiation hazard indices

$H_{ex}$  was calculated to estimate the level of radiological risk due to NORMs and external exposure to NORMs.  $H_{ex}$  was calculated for the surface soil samples by the Eq. (5) (Krieger, 1981).

$$H_{ex} = \frac{A_{Ra}}{370} + \frac{A_{Th}}{259} + \frac{A_K}{4810} \quad (5)$$

$H_{in}$  was calculated to estimate the level of radiological risk due to NORMs and internal exposure to NORMs.  $H_{in}$  was calculated for the surface soil samples by Eq. (6). (Awad et al., 2022).

$$H_{in} = \frac{A_{Ra}}{185} + \frac{A_{Th}}{259} + \frac{A_K}{4810} \quad (6)$$

$H_{ex}$  and  $H_{in}$  values must be below unity to avoid radiation.

Excess lifetime cancer risk (ELCR)

ELCR gives the lifetime cancer risk probability from exposure to ionizing radiation in any population. ELCR was estimated using the following equation (Taqi & Namq, 2022):

$$ELCR = AEDE\ (\mu Sv\ y^{-1}) \times DL\ (y) \times RF\ (Sv^{-1}) \quad (7)$$

In the equation, AEDE: the annual effective dose equivalent, DL: the average duration (70 years), RF: fatal risk factor (0.057) (ICRP, 2007).

Annual gonadal dose equivalent (AGDE)

In UNSCEAR report (2010), especially the thyroid, bone marrow, skin and gonads are interested organs in radiation research. AGDE ( $\mu Sv\ y^{-1}$ ) is calculated to estimate the effect of ionizing radiation on these sensitive organs using the following relation (Hamideen, 2022; UNSCEAR, 2010):

$$AGDE\ (\mu Sv\ y^{-1}) = 3.09A_{Ra} + 4.18A_{Th} + 0.314A_K \quad (8)$$

Gamma Representative Level Index ( $I_\gamma$ )

$I_\gamma$  was estimated to assess the  $\gamma$  radiation hazard due to NORMs in surface soil samples.  $I_\gamma$  must be less than unity to avoid the radiation.  $I_\gamma$  was calculated using the following relation (Boukhenfouf & Boucenna, 2011):

$$I_\gamma = \frac{A_{Ra}}{150} + \frac{A_{Th}}{100} + \frac{A_K}{1500} \quad (9)$$

## Results and discussions

Activity concentrations

The activity concentrations of NORMs in the surface soil of Konya City are plotted in Fig. 2. Geographic

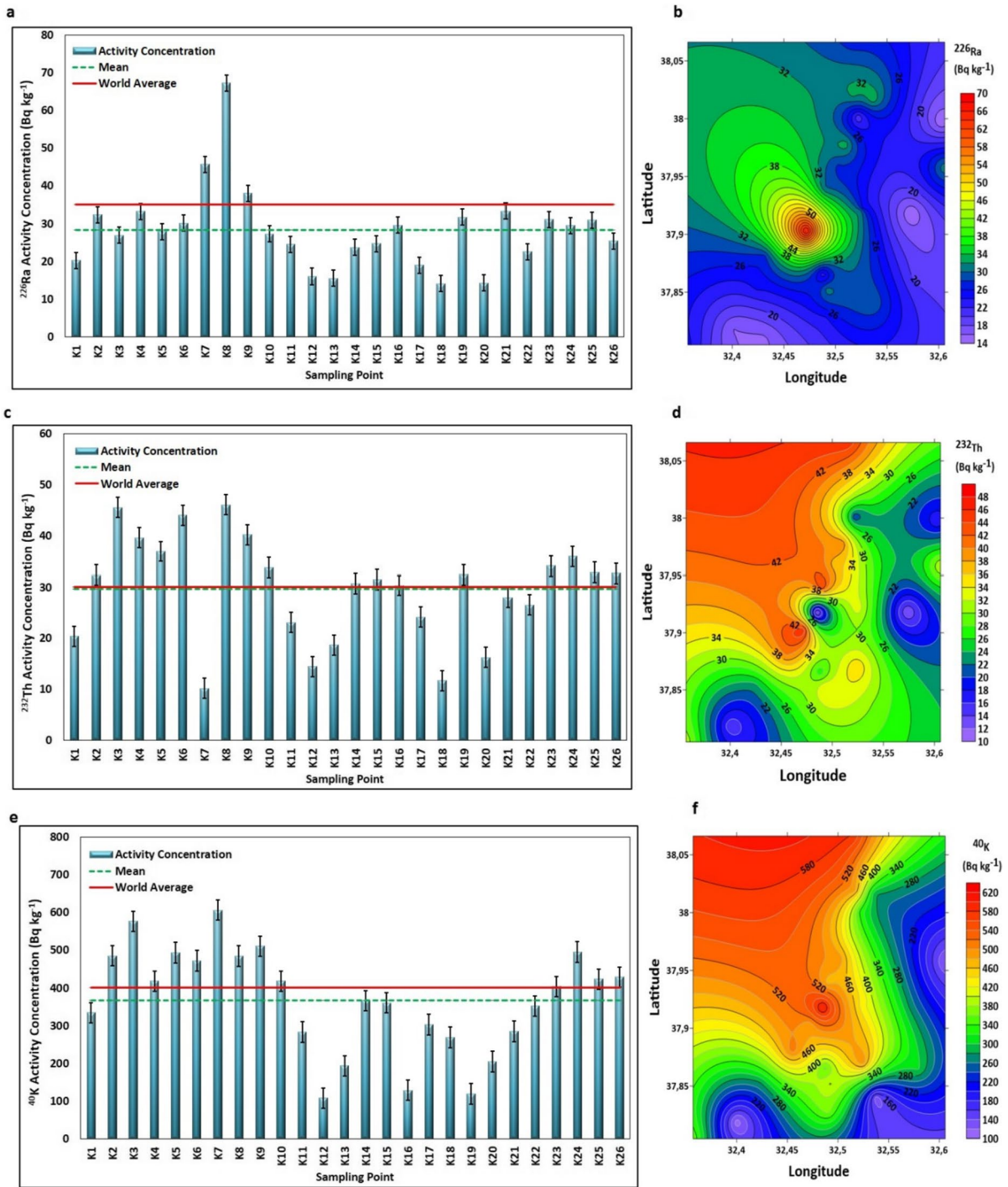


**Fig. 2** Activity concentrations of (a)  $^{226}\text{Ra}$ , (c)  $^{232}\text{Th}$ , (e)  $^{40}\text{K}$  and activity concentration distribution maps of (b)  $^{226}\text{Ra}$ , (d)  $^{232}\text{Th}$ , (f)  $^{40}\text{K}$

locations of collected soil samples and the obtained activity concentrations are listed in Table 1.

As can be seen in Table 1 and Fig. 2.a., the activity concentration of  $^{226}\text{Ra}$  was ranged from  $14.07 \pm 0.71$

**Table 1** Geographic locations and the activity concentrations of NORMs in Bq kg<sup>-1</sup>, dw

Sampling point	Geographic location		<sup>226</sup> Ra	<sup>232</sup> Th	<sup>40</sup> K
	N	E			
K1	38° 00' 04"	32° 31' 19"	20.21 ± 0.47	20.37 ± 1.01	334.12 ± 5.59
K2	38° 01' 10"	32° 31' 01"	32.36 ± 1.30	32.37 ± 2.36	484.89 ± 11.66
K3	38° 03' 58"	32° 30' 55"	26.91 ± 0.98	45.53 ± 0.70	576.61 ± 10.18
K4	37° 58' 39"	32° 30' 35"	33.18 ± 0.74	39.58 ± 2.28	417.84 ± 9.98
K5	37° 57' 36"	32° 30' 05"	27.83 ± 1.18	36.93 ± 1.68	493.27 ± 11.02
K6	37° 56' 24"	32° 29' 24"	30.10 ± 1.08	43.99 ± 0.78	471.64 ± 11.93
K7	37° 55' 04"	32° 29' 06"	45.69 ± 2.57	10.19 ± 2.60	605.95 ± 11.34
K8	37° 54' 10"	32° 28' 18"	67.27 ± 1.62	46.09 ± 0.76	484.32 ± 11.36
K9	37° 52' 50"	32° 27' 18"	38.06 ± 1.27	40.18 ± 0.72	510.67 ± 12.31
K10	37° 52' 51"	32° 25' 51"	27.26 ± 1.30	33.81 ± 0.75	417.88 ± 11.66
K11	37° 51' 14"	32° 25' 25"	24.46 ± 3.59	23.12 ± 0.96	283.13 ± 13.01
K12	37° 49' 07"	32° 23' 60"	15.97 ± 3.04	14.43 ± 0.88	107.87 ± 13.32
K13	37° 48' 33"	32° 25' 49"	15.47 ± 1.56	18.69 ± 1.01	193.00 ± 13.97
K14	37° 49' 39"	32° 29' 25"	23.71 ± 1.24	30.66 ± 1.11	365.92 ± 17.18
K15	37° 48' 16"	32° 21' 25"	24.64 ± 1.21	31.48 ± 0.79	360.24 ± 12.63
K16	37° 50' 25"	32° 32' 15"	29.56 ± 1.79	30.32 ± 1.86	128.37 ± 10.02
K17	37° 51' 54"	32° 34' 45"	18.92 ± 0.92	24.16 ± 0.59	302.83 ± 8.80
K18	37° 55' 07"	32° 34' 24"	14.07 ± 0.71	11.66 ± 0.50	268.34 ± 7.82
K19	37° 57' 28"	32° 36' 21"	31.72 ± 1.92	32.38 ± 1.04	118.64 ± 4.82
K20	37° 59' 48"	32° 36' 09"	14.23 ± 0.55	16.24 ± 0.31	204.51 ± 5.07
K21	38° 00' 59"	32° 32' 11"	33.30 ± 1.04	28.01 ± 0.60	284.68 ± 8.81
K22	37°51' 57"	32° 29' 16"	22.51 ± 1.06	26.52 ± 0.64	351.56 ± 10.54
K23	37°51' 06"	32° 29' 33"	31.11 ± 2.32	34.09 ± 1.26	403.33 ± 9.66
K24	37°52' 13"	32° 31' 28"	29.52 ± 1.03	35.95 ± 0.62	495.23 ± 10.93
K25	37°55' 12"	32° 31' 29"	30.91 ± 1.26	32.87 ± 0.69	423.23 ± 12.77
K26	37°55' 23"	32° 31' 35"	25.38 ± 2.58	32.68 ± 4.78	428.63 ± 8.73
Minimum	-	-	14.07 ± 0.71	10.19 ± 2.60	107.87 ± 13.32
Maximum	-	-	67.27 ± 1.62	46.09 ± 0.76	605.95 ± 11.34
Average	-	-	28.24 ± 1.47	29.70 ± 1.20	366.03 ± 10.58
World Average	-	-	35	30	400

Bq kg<sup>-1</sup> dw (sample K18) to 67.27 ± 1.62 Bq kg<sup>-1</sup> dw (K8). The average of activity concentration of <sup>226</sup>Ra was found as 28.24 ± 1.47 Bq kg<sup>-1</sup> dw. The average of activity concentration of <sup>226</sup>Ra is less than the world average. The <sup>226</sup>Ra activity concentrations for K7, K8 and K9 samples are higher than the world average. The activity concentration of <sup>232</sup>Th varied between 10.19 ± 2.60 Bq kg<sup>-1</sup> dw (K7) and 46.09 ± 0.76 Bq kg<sup>-1</sup> dw (K8) with an average value of 29.70 ± 1.20 Bq kg<sup>-1</sup> dw. The <sup>232</sup>Th activity concentrations for K2, K3, K4, K5, K6, K8, K9, K10, K15, K19, K23, K24, K25, and K26 samples are found higher than the world average (Fig. 2.c.). The activity concentration of <sup>40</sup>K was ranged from 107.87 ± 13.32

Bq kg<sup>-1</sup> dw (K12) to 605.95 ± 11.34 Bq kg<sup>-1</sup> dw (K7). The average of the activity concentration of <sup>40</sup>K was calculated as 366.03 ± 10.58 Bq kg<sup>-1</sup> dw. The average of the activity concentration of <sup>40</sup>K is lower than the world average (Fig. 2.e.). The <sup>40</sup>K activity concentrations for K2, K3, K4, K5, K6, K7, K8, K9, K10, K23, K24, K25, and K26 samples are found higher than the world average. The highest activity concentrations of NORMs in sampling points can be due to may be caused by the presence of industrial activities nearby and utilization of fertilizers in the soil (El Aouidi et al., 2021).

Activity concentration distribution maps are given in Fig. 2. Distribution maps of radionuclides were

**Table 2** Comparison of obtained natural radioactivity concentrations with other studies

Region	<sup>226</sup> Ra (Bq kg <sup>-1</sup> )	<sup>232</sup> Th (Bq kg <sup>-1</sup> )	<sup>40</sup> K (Bq kg <sup>-1</sup> )	References
North Cyprus	49.7–147.6	18.1–93.9	103.5–1468.6	(Abbasi et al., 2020)
Saudi Arabia	6–54	7–52	299–761	(Aydarous et al., 2022)
Seydisehir and Beysehir districts of Konya, Turkey	18–64	22–83	119–654	(Ozaydin Ozkara et al., 2021)
Istanbul, Turkey	19.97–50.80	21.38–52.61	464.06–711.27	(Günay, 2018)
Rize, Turkey	4.45–32.19	5.58–43.61	28.82–773.19	(Akçay, 2021)
İzmir, Turkey	23.5–59.5	37.5–64.4	354.7–978.4	(Özden & Aközcan, 2021)
Nevşehir, Turkey	7.40–193.90	<2.8–122.50	37.67–1370.20	(Bingöldağ & Otansev, 2020)
Egypt	6.6–37.1	2.9–55.7	37.0–873.5	(Salahel Din, 2022)
India	15.2–58	14–86.2	224.5–1650	(Srinivasa et al., 2022)
Namibia	7.74–20.04	8.59–31.74	108.8–484.9	(Hitila & Onjefu, 2022)
Laos	6.6–73.6	3.8–113.8	13.6–906.4	(Bui et al., 2020)
Iraq	4.4–34.7	1.5–13.3	42.1–583.9	(Smail et al., 2022)
Jordan	12.9–69.0	7.5–70.9	140.8–465.5	(Hamideen, 2022)
Yemen	22.73–39.95	50.4–94.95	924.57–1322.32	(El-Gamal et al., 2019)
Konya, Turkey	14.07–67.27	10.19–46.09	107.87–605.95	This study

plotted using the Surfer program (Golden Software Surfer 16). The highest activity concentrations can be seen as in red color in distribution maps and the lowest activity concentrations are in purple. The highest <sup>226</sup>Ra and <sup>232</sup>Th activity concentrations were observed at 37° 54' 10" N and 32° 28' 18" E. The highest <sup>40</sup>K activity concentration was observed at 37° 55' 04" N and 32° 29' 06" E.

Table 2 presents the comparison of the obtained natural radioactivity concentrations in this study with other studies in the world. Some activity concentration values of <sup>226</sup>Ra in the present study are lower than the studies in North Cyprus, Laos, Jordan, and Konya (Seydisehir-Beysehir districts, Turkey), while some values of <sup>226</sup>Ra are higher than that of Saudi Arabia, Konya (Seydisehir-Beysehir districts, Turkey), Istanbul (Turkey), Rize (Turkey), Izmir (Turkey), Egypt, India, Namibia, Iraq and Yemen. The highest value of <sup>232</sup>Th activity concentration is less than the highest value obtained in North Cyprus, Saudi Arabia, Konya (Seydisehir-Beysehir districts, Turkey), Istanbul (Turkey), Izmir (Turkey), Egypt, India, Laos, Jordan and Yemen. Similarly, the highest value of <sup>40</sup>K activity concentration is less than those of all compared studies except Namibia, Iraq and Jordan.

### Radiological hazard parameters

The radiological hazard parameters were evaluated for prospective radiological hazards to human health (Table 3).

Ra<sub>eq</sub> ranged from 44.91 to 170.47 Bq kg<sup>-1</sup> with a mean value of 98.90 Bq kg<sup>-1</sup>. All estimated Ra<sub>eq</sub> values are lower than the recommended permissible limit (370 Bq kg<sup>-1</sup>) (UNSCEAR, 2000). The minimum and the maximum values of D in the air due to the natural radionuclides were found as 20.59 and 79.11 nGy h<sup>-1</sup> respectively. In addition, the mean value of D was calculated as 46.25 nGy h<sup>-1</sup>. All calculated values of D except K3, K6, K8 and K9 sampling points are lower than the world average of 57 nGy h<sup>-1</sup>. AEDE ranged from 25.25 to 97.02 μSvy<sup>-1</sup>. The mean of AEDE was found as 56.73 μSvy<sup>-1</sup>. The worldwide average of AEDE is 70 μSvy<sup>-1</sup>. The mean of AEDE is lower than the world average, but AEDE values of some of the sampling points such as K3, K6, K8 and K9 are higher than the world average.

ELCR ranged from 0.10 × 10<sup>-3</sup> to 0.39 × 10<sup>-3</sup> with a mean of 0.23 × 10<sup>-3</sup>. The mean of ELCR value was obtained to be lower than the world average value (0.29 × 10<sup>-3</sup>). The highest and lowest values of all the calculated ELCR values appear at K8 and K12 sampling points, respectively. The ELCR values of K3, K6, K8 and K9

**Table 3** The obtained radiological hazard parameters

Sampling point	R <sub>a<sub>eq</sub></sub> (Bq kg <sup>-1</sup> )	D (nGy h <sup>-1</sup> )	AEDE (μSv y <sup>-1</sup> )	ELCR (10 <sup>-3</sup> )	H <sub>ex</sub>	H <sub>in</sub>	AGDE (mSv y <sup>-1</sup> )	I <sub>y</sub>
K1	75.07	35.57	43.63	0.17	0.20	0.26	0.25	0.56
K2	115.99	54.72	67.11	0.27	0.31	0.40	0.39	0.86
K3	136.42	63.98	78.46	0.31	0.37	0.44	0.45	1.02
K4	121.95	56.66	69.49	0.28	0.33	0.42	0.40	0.90
K5	118.62	55.73	68.35	0.27	0.32	0.40	0.40	0.88
K6	129.32	60.14	73.76	0.29	0.35	0.43	0.42	0.95
K7	106.92	52.53	64.42	0.26	0.29	0.41	0.37	0.81
K8	170.47	79.11	97.02	0.39	0.46	0.64	0.55	1.23
K9	134.84	63.15	77.44	0.31	0.36	0.47	0.45	1.00
K10	107.79	50.44	61.86	0.25	0.29	0.36	0.36	0.80
K11	79.32	37.07	45.46	0.18	0.21	0.28	0.26	0.58
K12	44.91	20.59	25.25	0.10	0.12	0.16	0.14	0.32
K13	57.06	26.48	32.48	0.13	0.15	0.20	0.19	0.42
K14	95.73	44.73	54.86	0.22	0.26	0.32	0.32	0.71
K15	97.39	45.42	55.70	0.22	0.26	0.33	0.32	0.72
K16	82.80	37.32	45.77	0.18	0.22	0.30	0.26	0.59
K17	76.79	35.96	44.10	0.18	0.21	0.26	0.25	0.57
K18	51.41	24.73	30.33	0.12	0.14	0.18	0.18	0.39
K19	87.16	39.16	48.03	0.19	0.24	0.32	0.27	0.61
K20	53.20	24.91	30.55	0.12	0.14	0.18	0.18	0.39
K21	95.27	44.17	54.17	0.22	0.26	0.35	0.31	0.69
K22	87.50	41.08	50.38	0.20	0.24	0.30	0.29	0.65
K23	110.92	51.78	63.51	0.25	0.30	0.38	0.37	0.82
K24	119.06	56.00	68.68	0.27	0.32	0.40	0.40	0.89
K25	110.50	51.78	63.51	0.25	0.30	0.38	0.37	0.82
K26	105.12	49.34	60.51	0.24	0.28	0.35	0.35	0.78
Minimum	44.91	20.59	25.25	0.10	0.12	0.16	0.14	0.32
Maximum	170.47	79.11	97.02	0.39	0.46	0.64	0.55	1.23
Mean	98.90	46.25	56.73	0.23	0.27	0.34	0.33	0.73

sampling points were found to be higher than the world average. The highest and the lowest values of AGDE were determined as 0.55 (K8 sampling point) and 0.14 mSv y<sup>-1</sup> (K12 sampling point) respectively. The mean AGDE value was found to be 0.33 mSv y<sup>-1</sup> which is slightly higher than the global limit value of 0.3 mSv y<sup>-1</sup>.

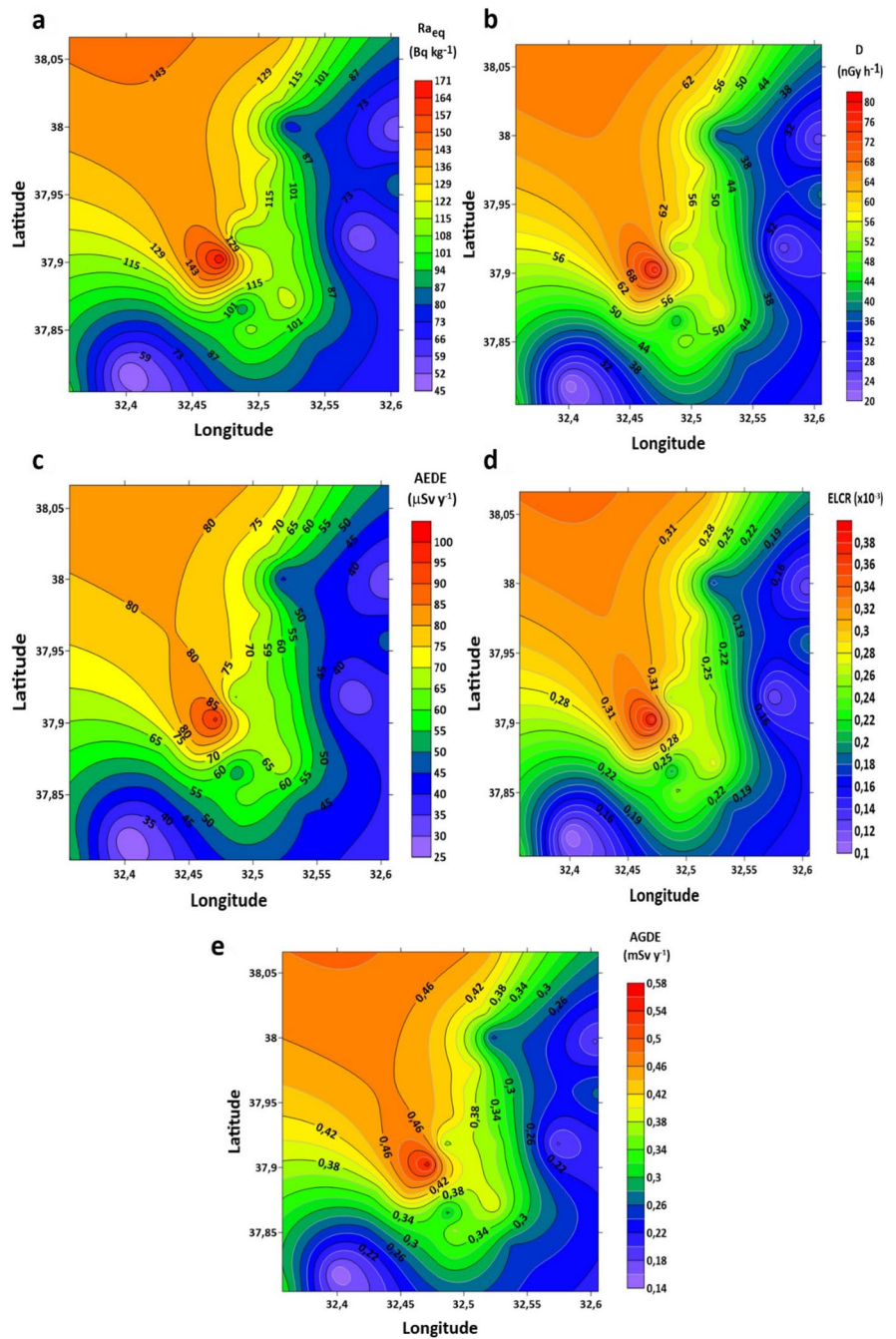
Radiological contour maps of R<sub>aeq</sub> (Bq kg<sup>-1</sup>), D (nGy h<sup>-1</sup>), AEDE (μSv y<sup>-1</sup>), ELCR (×10<sup>-3</sup>) and AGDE (mSv y<sup>-1</sup>) are shown in Fig. 3. Contour shapes and colors are quite similar to each other as seen on the maps. The highest radiological hazard parameters were observed at 37° 54' 10" N and 32° 28' 18" E. Higher radiological hazard parameters may be due to industrial activities, geological structure and geographical formation in the area.

H<sub>ex</sub>, H<sub>in</sub> and I<sub>y</sub> values and means of them are compared with a recommended permissible limit in Fig. 4. H<sub>ex</sub> ranged from 0.12 to 0.46 with a mean of 0.27. The highest and the lowest value of H<sub>in</sub> was found as 0.64 and 0.16, respectively. The mean of H<sub>in</sub> was calculated as 0.34. I<sub>y</sub> was found to vary from 0.32 to 1.23 with a mean value of 0.73. All calculated values of H<sub>in</sub> and H<sub>ex</sub> are found to be at a safe level, lower than the recommended permissible limit of 1. The mean values of H<sub>in</sub>, H<sub>ex</sub> and I<sub>y</sub> are below that of the unit limit. As seen in Fig. 4, the highest value of I<sub>y</sub> is above the recommended permissible limit of 1.

Cluster analysis (CA) was used to describe and classify variables with similar characters in the group. In cluster analysis, the similarity between



**Fig. 3** Radiological maps of (a)  $Ra_{eq}$  ( $Bq\ kg^{-1}$ ), (b)  $D$  ( $nGy\ h^{-1}$ ), (c) AEDE ( $\mu Sv\ y^{-1}$ ), (d) ELCR ( $\times 10^{-3}$ ) and e. AGDE ( $mSv\ y^{-1}$ )



the variables is evaluated depending on the distance between the variables. While zero distance indicates 100% similarity between clusters, the similarity rate between clusters decreases as the distance increases. CA was performed using average linkage for activity concentrations of NORMs and radiological hazard parameters.

The dendrogram is shown in Fig. 5. In the dendrogram, activity concentrations and radiological hazard parameters were grouped into three clusters. Cluster-I includes  $^{226}Ra$ ,  $^{232}Th$  and all radiological hazard parameters except  $Ra_{eq}$ . The reason why radiological hazard parameters are found in Cluster-1 is that radium and thorium have high activity in soil samples.

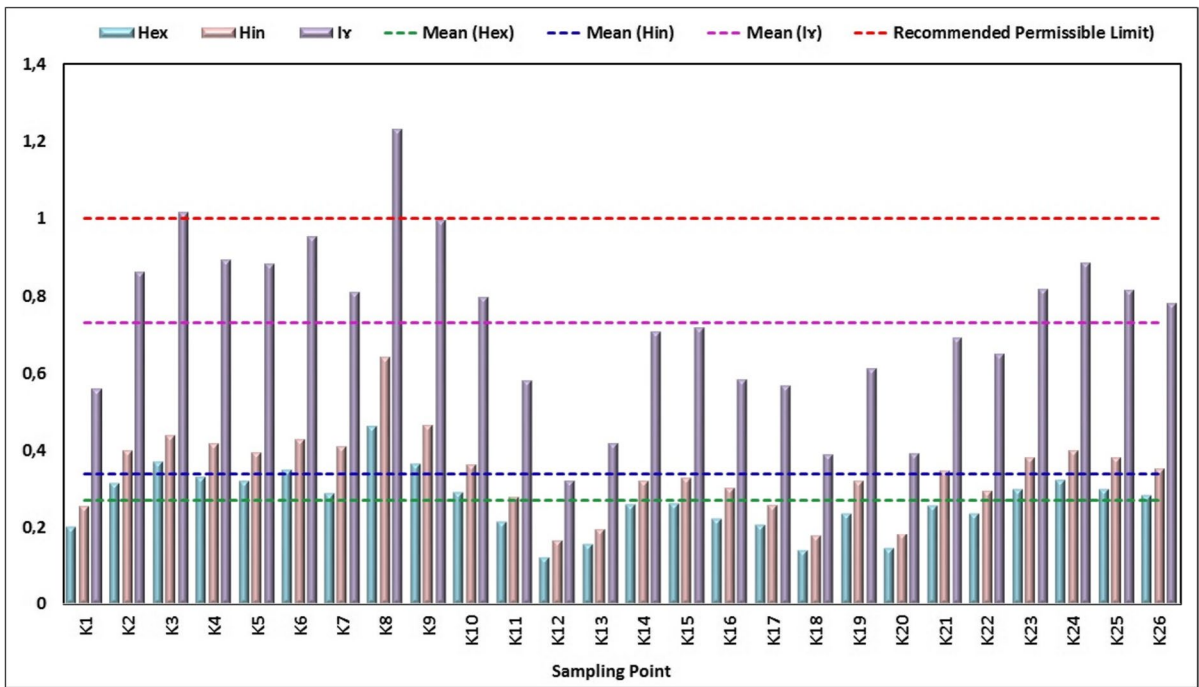
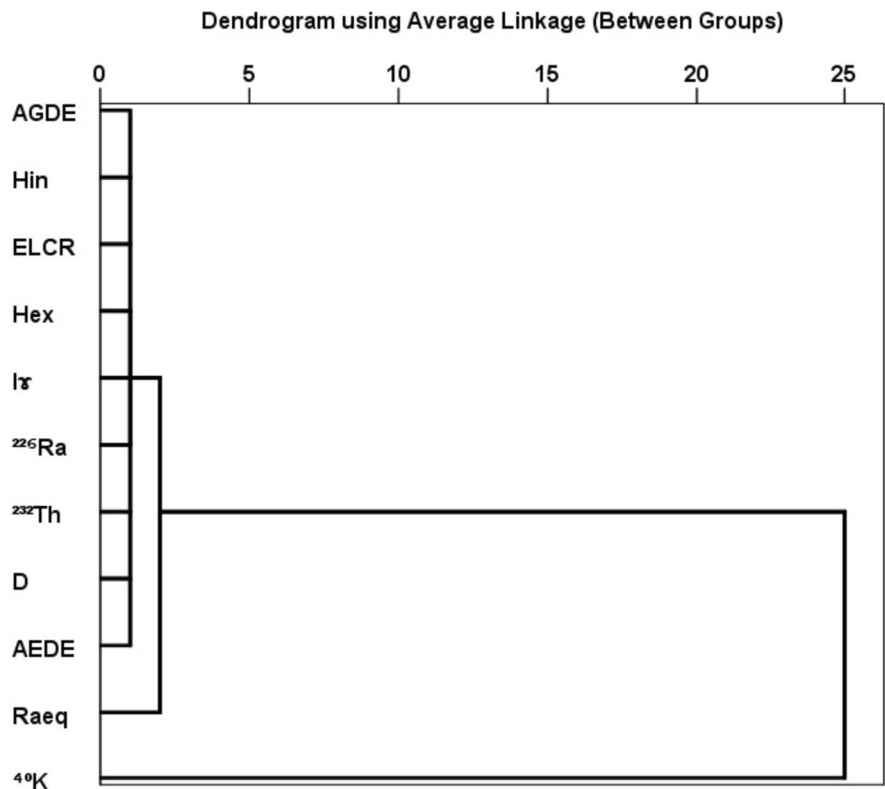


Fig. 4  $H_{ex}$ ,  $H_{in}$  and  $I_v$  for surface soil samples

Fig. 5 Dendrogram using average linkage



## Conclusion

The natural radioactivity concentrations in soil samples are determined for Konya city in Turkey. Using the coordinates in the studied area, mapping was made for activity concentrations and radiological hazard parameters. The average activity concentrations are lower than the world average value. In some regions of Konya, activity concentrations of  $^{226}\text{Ra}$ ,  $^{232}\text{Th}$ , and  $^{40}\text{K}$  were higher than the world average. The reason for this may be industrialization, and the use of artificial fertilizers in those areas. The radiological hazard parameters were calculated, and compared with world average values and recommended permissible limits. The mean value of  $\text{Ra}_{\text{eq}}$  is lower than the recommended permissible limit. In addition, the mean values of D, AEDE and ELCR are lower than the world average value but the mean value of AGDE is slightly higher than the global limit value in this study. The mean values of  $H_{\text{in}}$ ,  $H_{\text{ex}}$  and  $I_{\text{y}}$  are below that of the unit limit. CA was used to classify variables. In CA analysis, radiological hazard parameters were found in Cluster-1. This is because radium and thorium have high activity in soil samples.

**Acknowledgements** Use of facilities at the Central Research Laboratory of Kırklareli University for HPGe detector is acknowledged.

**Author contribution** Sample collection was performed by Osman Günay. Sample preparation, data counting, and data analysis were performed by Selin Özden and Serpil Aközcan Pehlivanoglu. The first draft of the manuscript was written by Selin Özden, Serpil Aközcan Pehlivanoglu and Osman Günay. Selin Özden, Serpil Aközcan Pehlivanoglu and Osman Günay checked the overall manuscript. All authors approved the final manuscript.

**Data availability** All data were presented in the manuscript.

## Declarations

**Ethics approval** All authors have read, understood, and have complied as applicable with the statement on “Ethical responsibilities of Authors” as found in the Instructions for Authors.

**Conflict of interest** The authors declare no competing interests.

## References

Abbasi, A., Kurnaz, A., Turhan, Ş., & Mirekhtiary, F. (2020). Radiation hazards and natural radioactivity levels in surface soil samples from dwelling areas of North Cyprus. *Journal of Radioanalytical and Nuclear Chemistry*, 324, 203–210. <https://doi.org/10.1007/s10967-020-07069-w>

Akçay, N. (2021). On the 30th anniversary of the Chernobyl Nuclear Power Plant Accident, assessment of the activity concentrations and the radiological hazard parameters of soil samples collected from Rize province and districts. *Applied Radiation and Isotopes*, 168, 109435. <https://doi.org/10.1016/j.apradiso.2020.109435>

Akkurt, İ., Gunoglu, K., Gunay, O., & Sarihan, M. (2022). Natural radioactivity and radiological damage parameters for soil samples from Cekmekoy-Istanbul. *Arabian Journal of Geosciences*, 15(1), 53. <https://doi.org/10.1007/s12517-021-09351-x>

Aközcan, S., Külahcı, F., Günay, O., & Özden, S. (2021). Radiological risk from activity concentrations of natural radionuclides: Cumulative Hazard Index. *Journal of Radioanalytical and Nuclear Chemistry*, 327, 105–122. <https://doi.org/10.1007/s10967-020-07474-1>

Al-Alawy, I. T., Taher, W. I., & Mzher, O. A. (2023). Soil radioactivity levels, radiation hazard assessment and cancer risk in Al-Sadr City, Baghdad Governorate, Iraq. *International Journal of Radiation Research*, 21(2), 293–298. <https://doi.org/10.52547/ijrr.21.2.16>

Alsaadi, S., Hazawi, A., & Elmzainy, A. S. (2023). Assessment of radioactivity in the soil samples from Al Bayda city, Libya, and its radiological implications. *Scientific Journal for Faculty of Science-Sirte University*, 3(1), 18–23. <https://doi.org/10.37375/sjfsu.v3i1.1058>

Awad, M., El Mezayen, A. M., El Azab, A., Alfi, S. M., Ali, H. H., & Hanfi, M. Y. (2022). Radioactive risk assessment of beach sand along the coastline of Mediterranean Sea at El-Arish area, North Sinai, Egypt. *Marine Pollution Bulletin*, 177, 113494. <https://doi.org/10.1016/j.marpolbul.2022.113494>

Aydarous, A., Zeghib, S., Abdullahi, S., & Al-Subaie, H. (2022). Radiological hazard assessment and sensitivity analysis for soil samples in Taghdoua area of Ranyah, Saudi Arabia. *Journal of Radiation Research and Applied Science*, 15(2), 119–128. <https://doi.org/10.1016/j.jrras.2022.05.006>

Beretka, J., & Mathew, P. J. (1985). Natural radioactivity of Australian building materials, industrial wastes and by-products. *Health Physics*, 48(1), 87–95.

Bingöldağ, N., & Otansev, P. (2020). Spatial distribution of natural and artificial radioactivity concentrations in soil samples and statistical approach, Nevşehir, Turkey. *Radiochimica Acta*, 108(11), 913–921. <https://doi.org/10.1515/ract-2020-0061>

Boukhenfouf, W., & Boucenna, A. (2011). The radioactivity measurements in soils and fertilizers using gamma spectrometry technique. *Journal of Environmental Radioactivity*, 102(4), 336–339. <https://doi.org/10.1016/j.jenvrad.2011.01.006>

Bui, V. L., Leuangtakoun, S., Bui, T. H., Vu, T. K. D., Le, T. N., Duong, T. D., Singsoupho, S., & Tran, H. N. (2020). Natural radioactivity and radiological hazards in soil samples in Savannakhet province, Laos. *Journal of Radioanalytical and Nuclear Chemistry*, 323(1), 303–315. <https://doi.org/10.1007/s10967-019-06965-0>

El Aouidi, S., Benmhammed, A., Benkdad, A., Mejjad, N., Toth-Bodrogi, E., Kovács, T., & Laïssaoui, A. (2021). Transfer of  $^{40}\text{K}$ ,  $^{226}\text{Ra}$  and  $^{210}\text{Pb}$  from soil to plants in various locations of El-Jadida agricultural area

- (north-western Morocco). In *E3S Web of Conferences* (Vol. 314, p. 01004). EDP Sciences. <https://doi.org/10.1051/e3sconf/202131401004>
- El-Gamal, H., Hussien, M. T., & Saleh, E. E. (2019). Evaluation of natural radioactivity levels in soil and various foodstuffs from Delta Abyan, Yemen. *Journal of Radiation Research and Applied Science*, *12*(1), 226–233. <https://doi.org/10.1080/16878507.2019.1646523>
- Elsaman, R., Seleem, E. M., Salman, S. A., Ella, E. E., & El-Taher, A. (2022). Evaluation of natural radioactivity levels and associated radiological risk in soil from Siwa Oasis, Egypt. *Radiochemistry*, *64*(3), 409–415. <https://doi.org/10.1134/S1066362222030195>
- Günay, O. (2018). Assessment of lifetime cancer risk from natural radioactivity levels in Kadikoy and Uskudar District of Istanbul. *Arabian Journal of Geosciences*, *11*, 1–6. <https://doi.org/10.1007/s12517-018-4151-9>
- Hafızoğlu, N. (2023). Radioactivity transfer factors and distribution of the natural and anthropogenic radionuclides in tea, plant and soil samples from the Black Sea Region in Turkey. *The European Physical Journal Plus*, *138*(4), 353. <https://doi.org/10.1140/epjp/s13360-023-03966-7>
- Hamideen, M. S. (2022). Correlations study between environmental radioactivity concentrations and some health risk indicators of soil samples in Amman city, Jordan. *International Journal of Environmental Analytical Chemistry*, *102*(2), 380–390. <https://doi.org/10.1080/03067319.2020.1722812>
- Hitila, M. V., & Onjefu, S. A. (2022). Natural radioactivity & associated radiological health hazards in soil around Van Eck Power plant. *arXiv preprint*, arXiv:2205.15854. 10.48550/arXiv.2205.15854
- Hossain, M. K., Hossain, S. M., Azim, R., & Meaze, A. M. H. (2010). Assessment of radiological contamination of soils due to shipbreaking using HPGe digital gamma-ray spectrometry system. *Journal of Environmental Protection*, *1*(1), 10. <https://doi.org/10.4236/jep.2010.11002>
- Ibraheem, A. A., El-Taher, A., & Alruwaili, M. H. (2018). Assessment of natural radioactivity levels and radiation hazard indices for soil samples from Abha, Saudi Arabia. *Results in Physics*, *11*, 325–330. <https://doi.org/10.1016/j.rinp.2018.09.013>
- Içhedef, M., Saç, M. M., Camgöz, B., Bolca, M., Demirel, N., & Oruç, Ö. E. (2015). Natural radioactivity levels of great soil groups in Seferihisar Geothermal Region, Turkey. *Environmental Earth Sciences*, *74*, 6283–6292. <https://doi.org/10.1007/s12665-015-4652-8>
- ICRP Publication 103. (2007). The 2007 Recommendations of the International Commission on Radiological Protection. *Annals of the ICRP*, *37*, 2–4.
- Krieger, R. (1981). Radioactivity of construction materials. *Betonwerk und Fertigteil Technik*, *47*(8), 468–473.
- Küçükönder, E., Gümbür, S., Söğüt, Ö., & Dođru, M. (2023). Natural radioactivity in soil samples taken from Kahramanmaraş provincial center. *Environmental Geochemistry and Health*, *45*, 5245–5259. <https://doi.org/10.1007/s10653-023-01577-w>
- Murthuza, K. M., Surumbarkuzhali, N., Thirukumaran, V., Gandhi, M. S., Ravi, A., Ganesh, D., & Ravisankar, R. (2022). Statistical analysis of natural radioactivity measurements for the soil of Tiruvannamalai District, Tamilnadu, India. *Materials Today: Proceedings*, *65*, 2606–2614. <https://doi.org/10.1016/j.matpr.2022.04.878>
- Murugesan, S., Mullainathan, S., Ramasamy, V., & Meenakshisundaram, V. (2011). Radioactivity and radiation hazard assessment of Cauvery River, Tamilnadu, India. *Iranian Journal of Radiation Research*, *8*(4), 211–222.
- Ozaydin Ozkara, R., Eke, C., & Boztosun, I. (2021). A study on the activity concentrations of <sup>226</sup>Ra, <sup>232</sup>Th, <sup>40</sup>K, <sup>137</sup>Cs and radiological risk assessments in soil samples from Seydisehir and Beysehir districts of Konya in Turkey. *Journal of Radioanalytical and Nuclear Chemistry*, *330*, 1017–1025. <https://doi.org/10.1007/s10967-021-08046-7>
- Özden, S. (2022). Assessment of natural radioactivity levels and radiological hazard parameters of soils collected from Bulgaria–Turkey border region. *The European Physical Journal Plus*, *137*(12), 1368. <https://doi.org/10.1140/epjp/s13360-022-03608-4>
- Özden, S., & Aközcan, S. (2021). Natural radioactivity measurements and evaluation of radiological hazards in sediment of Aliğa Bay, İzmir (Turkey). *Arabian Journal of Geosciences*, *14*, 1–14. <https://doi.org/10.1007/s12517-020-06446-9>
- Polat, A. T., & Önder, S. (2004). Urban park concept and an urban park sample for Konya. *Selcuk Journal of Agriculture and Food Sciences*, *18*(34), 76–86.
- Pucha, G., Pérez, M., Aguay, D., Chávez, E., Chávez, N., Giroletti, E., & Recalde, C. (2023). Soil radioactivity in the highest volcanic region of Northern Andes. *Journal of Environmental Radioactivity*, *262*, 107142. <https://doi.org/10.1016/j.jenvrad.2023.107142>
- Salahel Din, K. (2022). Soil radioactivity levels and radiation exposure to the population in Aswan and Abu Simbel areas, South of Egypt. *Physics and Chemistry of the Earth*, *127*. <https://doi.org/10.1016/j.pce.2022.103179>
- Şireci, N., Aslan, G., & Cakir, Z. (2021). Long-term spatiotemporal evolution of land subsidence in Konya metropolitan area (Turkey) based on multisensor SAR data. *Turkish Journal of Earth Sciences*, *30*(5), 681–697. <https://doi.org/10.3906/yer-2104-22>
- Smail, J. M., Ahmad, S. T., & Mansour, H. H. (2022). Estimation of the natural radioactivity levels in the soil along the Little Zab River, Kurdistan Region in Iraq. *Journal of Radioanalytical and Nuclear Chemistry*, *331*, 119–128. <https://doi.org/10.1007/s10967-021-08064-5>
- Solgun, E., Horasan, B. Y., & Ozturk, A. (2021). Heavy metal accumulation and potential ecological risk assessment in sediments from the southwestern Konya district (Turkey). *Arabian Journal of Geosciences*, *14*(8), 730. <https://doi.org/10.1007/s12517-021-07088-1>
- Srinivasa, E., Rangaswamy, D. R., Suresh, S., & Sannappa, J. (2022). Natural radioactivity levels and associated radiation hazards in soil samples of Chikkamagaluru district, Karnataka, India. *Journal of Radioanalytical and Nuclear Chemistry*, *331*, 1899–1906. <https://doi.org/10.1007/s10967-021-08133-9>
- Suresh, S., Rangaswamy, D. R., Sannappa, J., & Srinivasa, E. (2021). Gamma dose rate and annual effective dose equivalent in Uttara Kannada District, Karnataka, India. *Radiochemistry*, *63*, 672–681. <https://doi.org/10.1134/S1066362221050179>

- Taqi, A., & Namq, B. F. (2022). Radioactivity and radionuclide distribution in Jabel Bawr oil site of Kirkuk-Iraq. *Arab Journal of Nuclear Sciences and Applications*, 55(2), 113–124. <https://doi.org/10.21608/AJNSA.2021.93425.1508>
- Tiomene, D. F., Bongue, D., Guembou Shouop, C. J., Ngwa Ebongue, A., Penabei, S., Mbogning Feudjio, W., & Kwato Njock, M. G. (2023). Environmental impact assessment and statistical analysis of natural radioactivity in the slopes of Mount Cameroon area. *Arabian Journal of Geosciences*, 16(7), 413. <https://doi.org/10.1007/s12517-023-11511-0>
- UNSCEAR, (1993). Report, United Nations scientific committee on the effects of atomic radiation sources, effects and risks of ionizing radiations. .
- UNSCEAR. (2000). Exposures from Natural Sources, 2000 Report to General Assembly. Annex B, New York.
- UNSCEAR. (2010). *Sources and effects of ionizing radiation: Report to the General Assembly, with scientific annexes* (Vol. 1, pp. 1–219).
- Uosif, M. A. M., & El-Taher, A. (2008). Radiological assessment of Abu-Tartur phosphate, western desert Egypt. *Radiation Protection Dosimetry*, 130(2), 228–235. <https://doi.org/10.1093/rpd/ncm502>
- Žak, A., Isajenko, K., Piotrowska, B., Kuczbajska, M., Ząbek, A., & Szczygielski, T. (2010). Natural radioactivity of wastes. *Nukleonika*, 55, 387–391.

**Publisher's Note** Springer Nature remains neutral with regard to jurisdictional claims in published maps and institutional affiliations.

Springer Nature or its licensor (e.g. a society or other partner) holds exclusive rights to this article under a publishing agreement with the author(s) or other rightsholder(s); author self-archiving of the accepted manuscript version of this article is solely governed by the terms of such publishing agreement and applicable law.